May 2004

Characterization of Human UDP-glucose Dehydrogenase: CYS-276 Is Required for the Second of Two Successive Oxidations

Brandi J. Sommer
University of Nebraska - Lincoln

Joseph J. Barycki
University of Nebraska - Lincoln, jbarycki2@unl.edu

Melanie A. Simpson
University of Nebraska - Lincoln, msimpson2@unl.edu

Published in *The Journal of Biological Chemistry* **279**:22 (May 28, 2004), pp. 23590–23596. DOI:10.1074/jbc.M401928200 Available online at http://www.jbc.org/

Submitted for publication, February 22, 2004; published online March 24, 2004.

This work was supported by National Institutes of Health Award IP20 RR18759 (to M. A. S.).

Characterization of Human UDP-glucose Dehydrogenase: CYS-276 Is Required for the Second of Two Successive Oxidations

Brandi J. Sommer, Joseph J. Barycki, and Melanie A. Simpson*

Department of Biochemistry, University of Nebraska–Lincoln, Lincoln, Nebraska 68588-0664

* Corresponding author: Dept. of Biochemistry, University of Nebraska–Lincoln, N241 Beadle Center, Lincoln, NE 68588-0664. Tel.: 402-472-9309; Fax: 402-472-7842; Email: msimpson2@unl.edu

Abstract: UDP-glucose dehydrogenase (UGDH) catalyzes two oxidations of UDP-glucose to yield UDP-glucuronic acid. Pathological overproduction of extracellular matrix components may be linked to the availability of UDP-glucuronic acid; therefore UGDH is an intriguing therapeutic target. Specific inhibition of human UGDH requires detailed knowledge of its catalytic mechanism, which has not been characterized. In this report, we have cloned, expressed, and affinity-purified the human enzyme and determined its steady state kinetic parameters. The human enzyme is active as a hexamer with values for K_m and V_{max} that agree well with those reported for a bovine homolog. We used crystal coordinates for *Streptococcus pyogenes* UGDH in complex with NAD^+ cofactor and UDP-glucose substrate to generate a model of the enzyme active site. Based on this model, we selected Cys-276 and Lys-279 as likely catalytic residues and converted them to serine and alanine, respectively. Enzymatic activity of C276S and K279A point mutants was not measurable under normal assay conditions. Rate constants measured over several hours demonstrated that K279A continued to turn over, although 250-fold more slowly than wild type enzyme. C276S, however, performed only a single round of oxidation, indicating that it is essential for the second oxidation. This result is consistent with the postulated role of Cys-276 as a catalytic residue and supports its position in the reaction mechanism for the human enzyme. Lys-279 is likely to have a role in positioning active site residues and in maintaining the hexameric quaternary structure.

Abbreviations: UGDH, UDP-glucose dehydrogenase; FPLC, fast protein liquid chromatography

Introduction

UDP-glucose dehydrogenase (UGDH) catalyzes the conversion of UDP-glucose to UDP-glucuronic acid, an essential precursor for synthesis of extracellular matrix polysaccharides in numerous diverse species, including humans. The normal cellular functions of UGDH have been studied extensively in various organisms by targeted gene disruptions, and these studies demonstrate its importance in developmental processes. In *Drosophila melanogaster*, the enzyme is encoded by the *sugarless* gene and is required for heparan sulfate modification of proteins that control wing formation (1). In *Caenorhabditis elegans*, UGDH fuels the production of glycosaminoglycans essential for vulval morphogenesis and embryonic development (2). In zebrafish, the enzyme is critical for normal cardiac development (3), and the phenotype of targeted disruption is extremely similar to the murine HAS2 null (4); both phenotypes are lethal. Human and mouse HAS2 proteins are 97% identical and are responsible for production of hyaluronan at specific developmental stages (5). Because UGDH provides the requisite UDP-glucuronic acid precursor for hyaluronan synthesis, it is not surprising that UGDH null and HAS2 null would exhibit similar developmental impairments.

Hyaluronan is an extracellular matrix component that is involved directly in promoting normal cellular growth and migration, but its elevated production has been extensively implicated in the progression of epithelial cancers such as breast (6), colon (7), and prostate (8). Such elevated synthesis of hyaluronan places increased demand on intracellular UDP-glucuronic acid concentrations, which also must be increased to compensate. Inhibition of hyaluronan synthesis recently has been shown to reduce tumor angiogenesis and thereby restrict *in vivo* growth of human prostate tumors (9). Restriction of precursor availability by inhibition of UGDH may regulate the production of hyaluronan in tumors and therefore is a possible novel avenue for therapeutic intervention. Interestingly, UGDH was identified in breast cancer cells as a gene product dramatically up-regulated in response to elevated androgen (10), so an androgen-secreting organ such as the prostate may have a mechanism for increased UGDH expression. Although a clone of human UGDH has been reported (11), kinetic properties and detailed mechanistic characterization of the purified enzyme (a necessary prelude to inhibitor design) are not available yet.

Kinetic studies of the bovine (12–20), streptococcal (21–24), and plant (25, 26) enzymes have been reported. All forms of the enzyme are known to catalyze the same reaction. Two successive oxidations are performed by the enzyme to convert the 6'-hydroxyl of UDP-glucose to a carboxylate concurrent with reduction of 2 mol of NAD^+ to NADH. Early experiments to determine an enzyme mechanism in the bovine system preceded the availability of sequence information, so specific catalytic residues were not identified. However, results of these studies led to the interesting mechanism proposed in Scheme 1 in which we have numbered key residues identified in our experiments. According to analysis of the bovine enzyme, in the first step the 6'-carbon of UDP-glucose is thought to be covalently attached in a Schiff base linkage with a lysine residue at the active site of the protein. There is evidence to suggest that this imine undergoes the first oxidation step yielding an aldimine intermediate that is not released from the protein. The aldimine is hydrolyzed/attacked by an active site cysteine to yield a thiohemiacetal that has been detected in both bovine and streptococcal enzyme systems. This intermediate then is oxidized a second time to produce a thioester, which is spontaneously

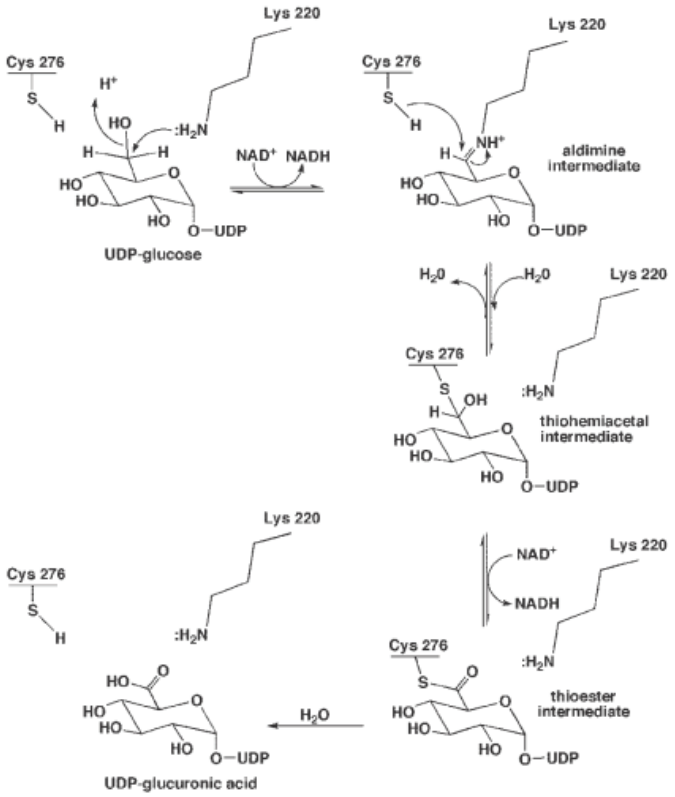

SCHEME 1

hydrolyzed to release UDP-glucuronic acid as a product. Hydrolysis of the thioester is thought to be rate-limiting overall. Notably, the streptococcal enzyme is believed to form a covalent intermediate specifically between the product of the first oxidation and cysteine 260 within the active site, which is required for the second oxidation. This residue is uniformly conserved across all species and corresponds to cysteine 276 in the human enzyme.

In this report, we have cloned, expressed, and purified recombinant human UGDH. To our knowledge, this is the first characterization of the human enzyme as well as the first mammalian UGDH to be purified and characterized by site-directed mutagenesis. We have determined that the enzyme is active as a hexamer with some evidence for assembly in a trimer of dimers as has been proposed for the bovine enzyme. Steady state kinetic constants were established and found to be comparable with previously published data in the bovine system. In addition, we generated a structural model of human UGDH based on the published crystal coordinates for the streptococcal homolog. Using this model and primary sequence alignments of known UGDH family members, we selected Cys-276 and Lys-279 as likely active site catalytic residues and converted them to serine and alanine, respectively. Enzymatic activity of C276S and K279A point mutants was not measurable under normal assay conditions. Rate constants were measured over several hours and demonstrated that K279A continued to turn over, although 250-fold more slowly than wild type enzyme. C276S, however, performed only a single round of oxidation indicating that it is essential for the second oxidation. This result is consistent with the postulated role of Cys-276 as a catalytic residue as shown in Scheme 1 and supports its position in the reaction mechanism for the human enzyme. Lys-279 appears to function structurally in preserving both the active site architecture and quaternary structure of the enzyme.

Experimental Procedures

Construction of Expression Vectors for Wild Type UGDH and Point Mutants—Reverse-transcribed poly(A)$^+$ RNA isolated from human prostate tumor cells was used as a template for PCR. Oligonucleotides were designed using the published sequence for human UGDH (Gen-Bank™ accession number AF061016) to incorporate an NheI restriction enzyme site immediately prior to the ATG start codon and a SalI site subsequent to the stop codon. The resultant 1.5-kb PCR product was digested with the relevant enzymes and ligated into similarly digested pET28a, a prokaryotic expression vector incorporating a cleavable N-terminal His tag (Novagen). Point mutants were generated using the QuikChange site-directed mutagenesis kit (Stratagene) following the manufacturer's protocol. Point mutant coding sequences were subcloned in pET28a. All subclones were sequenced by the Genomics Core at the University of Nebraska-Lincoln.

Expression and Purification of Wild Type and Mutant UGDH—The recombinant plasmids encoding N-terminal His_6 fusions to UGDH and the point mutants C276S and K279A were used to transform *Escherichia coli* strain Rosetta(DE3)pLysS (Novagen). Cultures were grown to an A_{600} of 0.6-0.8 in 2xYT media containing 34 mg/liter chloramphenicol and 30 mg/liter kanamycin at 30 °C and then were induced for 4 h by the addition of isopropyl-1-thio-β-D-galactopyranoside to a final concentration of 0.5 mM. The cells were harvested by centrifugation and resuspended in 50 mM sodium phosphate buffer, pH 8.0, containing 0.3M NaCl and 10 mM imidazole. Cells were lysed by sonication and centrifuged for 15 min at 15,000 $\times$ *g*. All three recombinant proteins were found to be expressed in the soluble fraction. The supernatant was treated with 0.35% (v/v) polyethyleneimine at 4 °C for 30 min and centrifuged for 15 min at 15,000 × *g* to separate precipitated nucleic acids from the protein-containing soluble fraction. The enzyme then was purified by affinity chromatography using a nickel-chelating column (Novagen) according to the manufacturer's protocol. Typical yields were 20-40 mg of purified protein per liter of bacterial culture. All preparations were >95% pure based upon SDS-PAGE (see Figure 1). The purified protein was dialyzed against 20 mM Tris-HCl, pH 7.4, and 1 mM dithiothreitol. By comparing uncleaved and thrombin-cleaved protein in the activity assay described below, we investigated whether the N-terminal His tag affected wild type enzyme activity. The His tag was cleaved by incubating the protein with 1 unit/mg thrombin (Novagen) for 1 6 h at 4 °C followed by dialysis against 20 mM Tris-HCl, pH 7.4, and 1 mM dithiothreitol. Cleavage of the tag was verified by SDS-PAGE. Cleaved and uncleaved proteins were found to have identical enzymatic activity. Protein storage conditions also were tested, and the protein, although stable at 4 °C for up to 48 h, was only stable long-term at –80 °C following flash freezing in a dry ice/acetone bath. Subsequent characterizations were performed exclusively, therefore, on aliquots of uncleaved protein stored in this fashion.

Enzymatic Activity Measurement and Kinetic Characterizations—Enzymatic activity of the wild type enzyme was determined by monitoring the change in absorbance at 340 nm that accompanies the reduction of NAD$^+$ to NADH. For standard screening of enzymatic activity, the assay was performed for 30 s at room temperature in 0.1 M Tris-HCl buffer, pH 7.4, containing 1 mM UDP-glucose (Fluka) and 10 mM NAD$^+$ (Sigma). The K_m and V_{max} for UDP-glucose and NAD$^+$ were determined independently using standard assay conditions. Constants for UDP-glucose as substrate were measured by holding NAD$^+$ constant and varying [UDP-glucose] from 0 to 200 μM. Similarly, NAD$^+$ kinetic measurements were made by holding UDP-glucose constant and varying NAD$^+$ from 0 to 2 mM. Triplicate values were obtained for each measurement, and data were plotted with Prism software (GraphPad). K_m and V_{max} were calculated by fitting the data to the Michaelis-Menten equation and assuming a single binding site each for substrate and cofactor.

Kinetic measurements for the two point mutants initially were made under standard assay conditions, and activity was found to be negligible at the 30-s time point. To determine whether residual enzymatic activity remained in these mutants, assays were set up with saturating cofactor and substrate, and an absorbance scan from 290 to 400 nm was collected every 5 min for 4 h. The resulting A_{340} values then were replotted over the time course of the assay and analyzed in Prism by fitting to a curve with a one-and two-phase exponential rate for C276S and K279A, respectively, to model the first and second oxidations of NAD$^+$.

Determination of Cofactor Binding Constants—To quantify cofactor binding independently of enzyme activity, intrinsic tryptophan fluorescence was measured. The wild type protein was scanned to determine the wavelength that gave maximum excitation (290 nm, data not shown); excitation at this value then was used to scan for maximum emission (335 nm). Each of the point mutants was scanned to verify equivalent excitation and emission

maxima. Intrinsic tryptophan fluorescence was monitored using these excitation and emission values in the presence of increasing NAD^+ from 0 to 1.5 mM. K_d values were obtained for each enzyme by fitting corrected fluorescence quenching to a curve with a single exponential decay (Prism).

Molecular Mass Determination—The functional molecular mass of the active UGDH enzyme complex was determined by gel filtration chromatography. Purified recombinant UGDH wild type and point mutants were individually loaded on a Superdex 200 HR 10/30 column (Amersham Biosciences) and separated by FPLC in 50 mM $NaPO_4$, pH 7.0, containing 150 mM NaCl, at a flow rate of 0.25 ml/min. Size determination was made by comparison with molecular weight standards (Amersham Biosciences) chromatographed under the same conditions. The molecular mass standards used (see *inset plot* of Figure 3) were as follows: thyroglobulin, 699 kDa; ferritin, 416 kDa; catalase, 219 kDa; aldolase, 176 kDa; albumin, 67 kDa; ovalbumin, 47 kDa; chymotrypsinogen A, 20 kDa; RNase A, 15 kDa. Resolution was sufficient to calculate molecular masses unambiguously in multiples of 57 kDa (the calculated molecular mass of monomeric His-tagged UGDH).

Homology Modeling and Portrayal of Active Site Residues—Human UGDH is 23% identical to the *Streptococcus pyogenes* enzyme for which a crystal structure has been published. We modeled human UGDH using 3D-PSSM (27), which superimposed the human amino acid sequence onto the Protein Data Bank coordinates for *S. pyogenes* UGDH (Protein Data Bank code 1DLI). A ribbon rendering of the model was made with Chimera (28). The active site was centered upon, and the model, in conjunction with sequence conservation, was used to select appropriate putative catalytic residues, which are depicted in Figure 4.

Results

Protein Expression and Purification—Although the cDNA for human UGDH was expressed previously in eukaryotic cells and the functionality implied by its nomenclature verified, no kinetic data were reported for the enzyme. Our goal was to measure steady state kinetic constants for wild type human UGDH, determine the subunit structure of the active enzyme complex, identify key active site residues, and assess the role of each in the enzyme mechanism. To facilitate these characterizations, wild type UGDH and specific point mutants each were subcloned in a bacterial expression vector that encoded an N-terminal 6-histidine fusion for affinity purification. The resultant constructs expressed abundant soluble recombinant UGDH in *E. coli*, and each enzyme form was purified to homogeneity by nickel affinity chromatography (Figure 1). To verify that the N-terminal histidine tag did not affect the structure or function of wild type UGDH or its mutants, the histidine tag was removed by thrombin cleavage, and the resulting protein was compared with uncleaved protein. Because cleaved and uncleaved proteins exhibited identical levels of enzyme activity (data not shown), uncleaved protein was used for subsequent characterizations.

Kinetic Characterization of UGDH—UGDH catalyzes conversion of a UDP-glucose substrate to a UDP-glucuronic acid product, concomitantly reducing two molecules of NAD^+ to NADH. The enzymatic activity of wild type UGDH was characterized by steady state kinetic analysis. To obtain kinetic constants (K_m and V_{max}) for substrate and cofactor, we measured the steady state level of NADH by its absorbance at 340 nm. Measurements to determine the dependence of the reaction on cofactor concentration were conducted using purified UGDH incubated with increasing concentrations of NAD^+ in the presence of saturating UDP-glucose substrate (Figure 2*A*). Similarly, dependence of reaction kinetics on substrate was measured by increasing UDP-glucose concentration in the presence of saturating NAD^+ (Figure 2*B*). Saturation kinetics were observed for both conditions. Data were fitted to the Michaelis-Menten equation to obtain K_m and V_{max} for the reaction catalyzed by the wild type enzyme (Table I). Both sets of conditions yielded a similar V_{max} of ≈120 nmol of NAD^+/min/mg of enzyme. The K_m for UDP-glucose was 11.2 μM, and the K_m for NAD^+ was 355 μM.

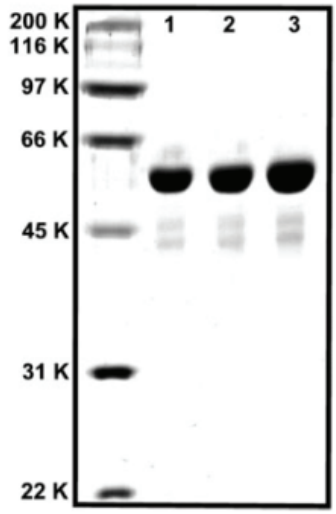

Figure 1. Purity of wild type and mutant UGDH. Recombinant His-tagged human UGDH and specified point mutants were overexpressed in *E. coli* and purified to homogeneity from the soluble extract in a single nickel affinity chromatography step. The purity of wild type UGDH (*lane 1*), C276S mutant (*lane 2*), and K279A mutant (*lane 3*) proteins was evaluated by SDS-PAGE followed by staining with GelCode Blue (Pierce). Proteins were judged to be >95% pure.

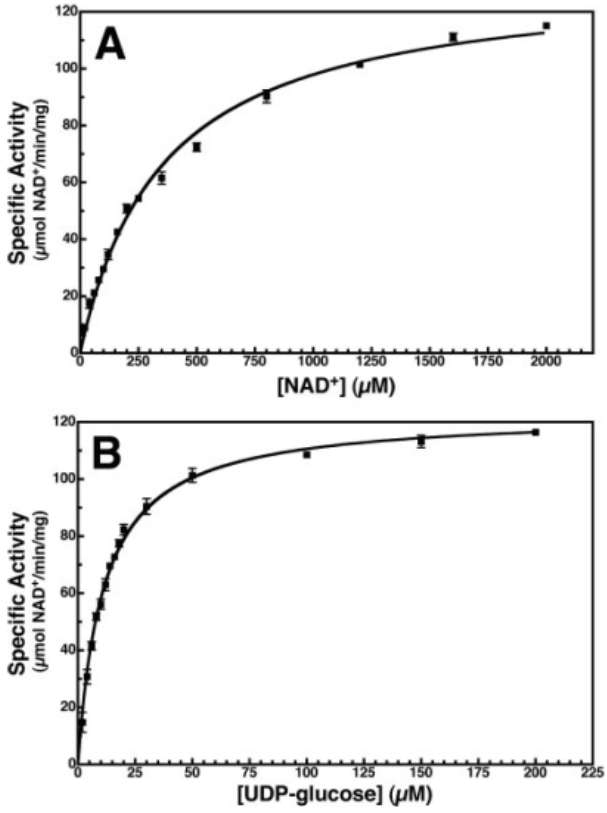

Figure 2. Wild type UGDH demonstrates saturable kinetics for NAD^+ (*A*) and UDP-glucose (*B*). Steady state enzyme activity was measured as conversion of NAD^+ to NADH detected by absorbance at 340 nm. Purified human UGDH (0.5 mg/ml in 0.1 M Tris-HCl, pH 7.4) was incubated for 1 min with increasing concentrations of NAD^+ (0-2 mM) in the presence of saturating substrate (*A*, UDP-glucose, 2 mM) or with increasing concentrations of UDP-glucose in the presence of saturating cofactor (*B*, NAD^+, 2 mM).

Characterization of UGDH Oligomeric State—Previous studies with *S. pyogenes* UGDH indicate that the enzyme is a dimer, but the bovine enzyme is considered to be hexameric. To determine the

Table I
Steady state kinetic constants for wild type UGDH

Substrate	K_m	V_{max}
	μM	*nmol/min/mg*
UDP-glucose	11.2 ± 0.28	118 ± 1.0
NAD^+	355 ± 12.4	128 ± 1.6

oligomeric state of human UGDH, we performed size exclusion analysis by FPLC (Figure 3). Consistent with data for the bovine ortholog, human UGDH predominantly is observed as a hexamer eluting from the gel filtration column at a molecular mass corresponding to six times the single subunit mass (*peak I*). Significant dimeric (*II*) and monomeric (*III*) species also are present, indicating some subunit dissociation. This elution profile was observed repeatedly over several different preparations of the enzyme with relative species ratios conserved so the distribution of subunit structures appears to be an innate property of the enzyme. The *inset panel* shows molecular weight determination for the peaks on the basis of size exclusion standards. The functional enzyme was analyzed independently by dynamic light scattering (data not shown), which estimated its molecular mass at 345 kDa (hydrodynamic radius of 7.2 nm) consistent with a hexameric assembly of the 57-kDa monomers.

Determination of UGDH Cofactor Binding Affinity—To characterize the initial binding of NAD^+ cofactor to UGDH independently of its apparent binding during 2-fold oxidation in turnover, we monitored the intrinsic tryptophan fluorescence of UGDH. We determined that fluorescence emission of the protein at 335 nm was quenched by the incremental addition of NAD^+ (data not shown). Tryptophan quenching was plotted as a function of NAD^+ concentration and fitted to an exponential decay assuming a single binding site (Prism). The resulting dissociation constant was 118 ± 3.3 μM (Table II). This value is comparable in order of magnitude to the K_m for NAD^+ determined by catalytic turnover.

Homology Modeling of UGDH—The structure for human UGDH has not been solved yet, but the human enzyme is 23% identical to its ortholog in *S. pyogenes* for which a structure was recently published. Using the coordinates of the bacterial enzyme complexed with cofactor and substrate, we modeled the human enzyme as a ternary complex with NAD^+ cofactor and UDP-glucose substrate and inspected the architecture of the active site (Figure 4). The degree of structural similarity was sufficient to identify specific residues in the human enzyme likely to participate in catalysis. Cys-260 of the streptococcal UGDH was mutagenized previously and found to reduce enzyme activity. Based on the homology model of human UGDH and previously published studies of the bacterial enzyme, we identified specific residues within the active site that were likely to be important for catalytic activity. We generated point mutations at residues Cys-276 (the human analog of Cys-260) and Lys-279 to investigate their individual contributions to the enzyme mechanism. Figure 4 illustrates the position of these two residues in the active site of the human UGDH model relative to NAD^+ and UDP-glucose. Also shown are side chains of residues Lys-220 and Asp-280 (see "Discussion").

Kinetic Characterization of UGDH Point Mutants—Catalytic activity of UGDH point mutants C276S and K279A initially was measured under standard reaction conditions and found to be negligible. For C276S, this observation is consistent with results of the analogous C260S streptococcal point mutant, which lacked activity to an unquantified degree. To evaluate the role of each residue in catalysis and determine the extent of impaired catalytic function, we performed a time course over 4 h, measuring enzyme activity every 5 min by absorbance wavelength scans from 290 to 400 nm. Conversion of NAD^+ to NADH by C276S (Figure 5*A*) was found to saturate at a concentration equimolar to that of added protein, suggesting that a single round of oxidation can occur in the absence of this cysteine but that the cysteine is essential for the second oxidation. In contrast, cofactor reduction was not saturable in the reaction catalyzed by the K279A mutant (Figure 5*B*), demonstrating its continued capacity for multiple turnover.

Absorbance values at 340 nm were replotted as a function of assay time to determine kinetic constants for the reaction (Figure 5*C*). As mentioned above, values for C276S were observed to plateau at an A_{340} of ≈0.17. This absorbance value corresponds to a 1:1 molar ratio of NADH produced relative to added protein. Under identical conditions, K279A continued to turn over without reaching an end point.

Saturable C276S kinetic data were fitted to an equation with a single rate for catalysis of ≈2.7 nmol of NAD^+/min/mg of enzyme (Table III). This value is ~50-fold diminished from the overall rate of NAD^+ turnover by wild type enzyme. Cys-276 therefore is not only essential for the second round of oxidation; it is also involved in efficient execution of the first round. Data replotted for K279A, which did not achieve saturation in the time course of the assay, revealed two rate constants. The first, k_1, was comparable with the rate constant for C276S (≈2.5 nmol/min/mg), but was followed by a much slower rate, k_2, of ≈0.4 nmol/min/mg. Hence, although not directly required for either oxidation, Lys-279 appears to have a global role in the catalytic function.

Cofactor Binding by Wild Type and Mutant UGDH—To verify that observed differences in enzyme activity among wild type and point mutants of UGDH were not attributable to a loss of cofactor binding, we compared intrinsic tryptophan quenching in the presence of increasing concentrations of NAD^+. Fluorescence emission was fitted to a saturation curve assuming a single binding site. Resultant dissociation constants (Table II) demonstrate comparable cofactor affinities among wild type and mutant UGDH (118, 127, and 103 μM for wild type, C276S, and K279A, respectively), suggesting that the folded structures of the mutant proteins were unaffected by the respective point mutation. Furthermore, loss of enzymatic activity was not the result of a change in binding of NAD^+ by either mutant despite the suggestive hydrogen bonding proximities illustrated by Figure 4 that might implicate Lys-279 in cofactor binding.

Subunit Association of Mutant UGDH—Because altered catalytic activity of the mutants also could result from changes in quaternary structure, the oligomeric state of the mutant enzymes was examined for perturbations by size exclusion FPLC. Whereas C276S retained a predominantly hexameric structure with a minor dimeric peak as compared by overlay of its elution profile on that of the wild type enzyme (Figure 6*A*), K279A is found almost exclusively as a dimer (Figure 6*B*). This observation is consistent with the UGDH quaternary structure adopting a "trimer of dimers" arrangement within the hexameric protein. Although the homology model of UGDH does not predict a surface exposed location for Lys-279, it appears to be required for maintenance of the trimer interfaces that must occur independently of dimerization.

Discussion

UGDH is expressed by most species from bacteria to humans. In plants and bacteria, its role is in the maintenance of structural integrity. In animals, its functional significance is developmental, and its dysregulation is linked indirectly to several pathologies, including cancer progression. Specific targeted inhibition of this enzyme may offer a therapeutic avenue but requires a detailed understanding of its

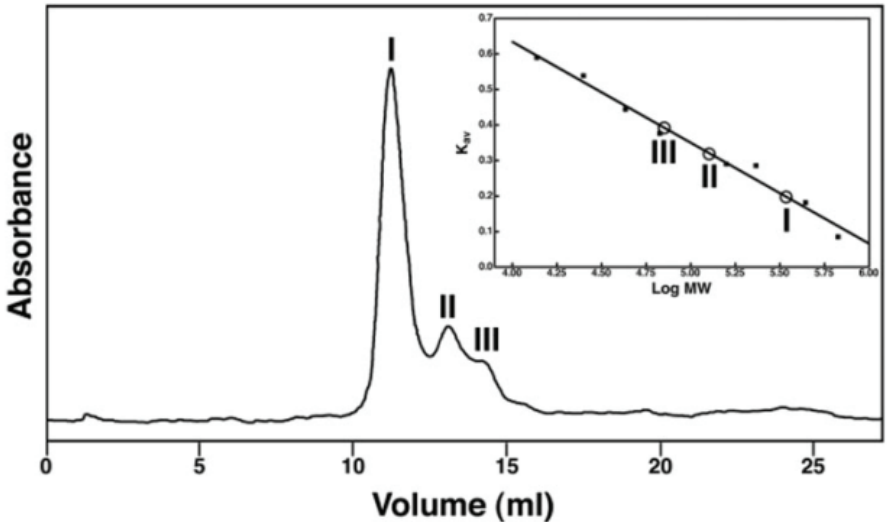

Figure 3. Wild type UGDH is active as a hexamer. Purified human UGDH was fractionated by gel filtration FPLC on a Superdex 200 HR 10/30 resin. One major and two minor peaks were detected as discussed in the text. Size determination was made by comparison with molecular weight standards fractionated under identical conditions. Average retention time in the column was plotted *versus* the log of the molecular weight for each standard (*inset*). Standards used were as follows: thyroglobulin, 699 kDa; ferritin, 416 kDa; catalase, 219 kDa; aldolase, 176 kDa; albumin, 67 kDa; ovalbumin, 47 kDa; chymotrypsinogen A, 20 kDa; RNase A, 15 kDa.

Table II
NAD^+ binding constants for wild type and mutant UGDH

Enzyme	K_d
	μM
UGDH	118 ± 3.3
C276S	127 ± 4.0
K279A	103 ± 3.0

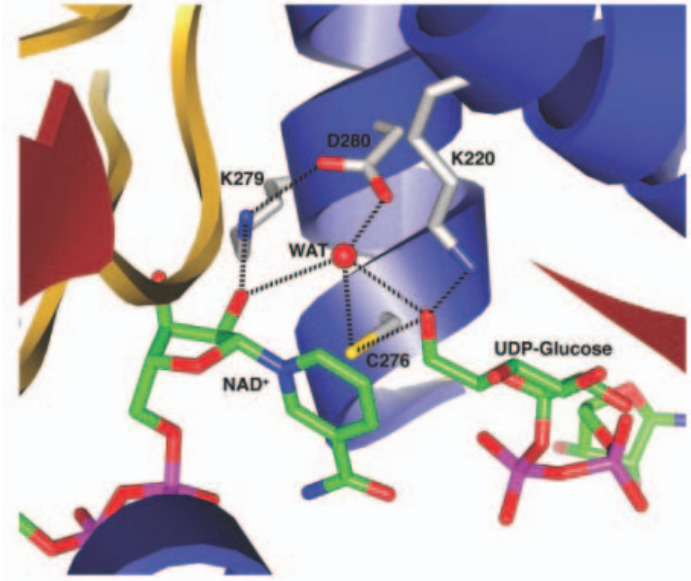

Figure 4. Active site model of the UGDH ternary complex. The human UGDH primary sequence was superimposed on the published crystal structure coordinates for the *S. pyogenes* enzyme (Protein Data Bank code 1DLI). A model was generated using 3D-PSSM and was represented in Chimera as a ribbon diagram. The model depicts the human enzyme in complex with NAD^+ cofactor and UDP-glucose substrate. Side chains of specific active site residues discussed in the text are shown. The network of hydrogen bonding between protein active site residues and the cofactor and substrate is illustrated by *dotted lines* (see "Discussion"). The coloring scheme is as follows: the overall helical ribbon is *blue* and the loops are *yellow*; within the active site, carbon atoms of the protein are *gray*, carbons in the cofactor and substrate are *green*, nitrogen is *blue*, oxygen is *red*, sulfur is *yellow*, and phosphorus is *pink*.

mechanism. To date, most mechanistic studies have focused on the bovine or bacterial forms of the enzyme. In the study we have presented here, human UGDH was cloned, expressed, and purified to homogeneity. We report the first characterization of its mechanistic features. Kinetic properties of the hexameric enzyme are comparable with those reported previously for UGDH orthologs. Specific point mutants were generated based on homology modeling of the enzyme and used to dissect the components of the enzyme reaction sequence. Cys-276 is required for the second but not the first of the two successive oxidations. Lys-279 is not an absolute requirement for activity, but mutation of this residue impairs catalysis and disrupts the quaternary structure of the protein. Its role probably is to position the active site cysteine for maximally efficient catalysis, but it may also be an important contact at the trimeric interface.

Human UGDH is closely related to the enzyme characterized from bovine liver but is only 23% identical to the *S. pyogenes* enzyme, both of which catalyze the same 2-fold oxidation of UDP-glucose to UDP-glucuronic acid, apparently by similar mechanisms. Not surprisingly, the kinetic activity and quaternary structure of the wild type human protein are very similar to the bovine; the kinetic constants we have measured are within 2-fold of those reported for the bovine enzyme, which also functions as a hexamer (16). The *S. pyogenes* enzyme, in contrast, is dimeric and has slightly lower binding constants for substrate and cofactor relative to both mammalian proteins (23). It is not clear what role subunit associations may play in enzyme function. Both substrate binding assays and chemical modifications of the active site cysteines in the bovine enzyme suggest that there is half-site reactivity among the subunits in the trimer of dimers that is induced through subunit communication following the first binding event (17, 20). This phenomenon may provide a regulatory mode for human and bovine UGDH. Although it is possible that the reduced activity of our K279A mutant is attributable to its altered subunit structure, we have additionally generated a point mutant, K339A, that also is dimeric but exhibits activity comparable with that of wild type (data not shown). Lys-279 is shown by the homology model to be located in a solvent-exposed stretch of helix adjacent to the dimerization interface. Evolutionarily speaking, the hypothesis has been put forth that the bacterial enzyme preceded the animal forms (11). The dimer interface then most likely would be conserved among species, and the contacts between dimers would be elsewhere. The quaternary structures of our lysine mutants are consistent with conserved localization of the dimer interface and predict that interdimer association occurs through contacts maintained, at least in part, by the solvent-exposed helix containing Lys-279.

Site-directed mutagenesis is a powerful tool with which to functionally dissect the roles of residues within an enzyme active site. To

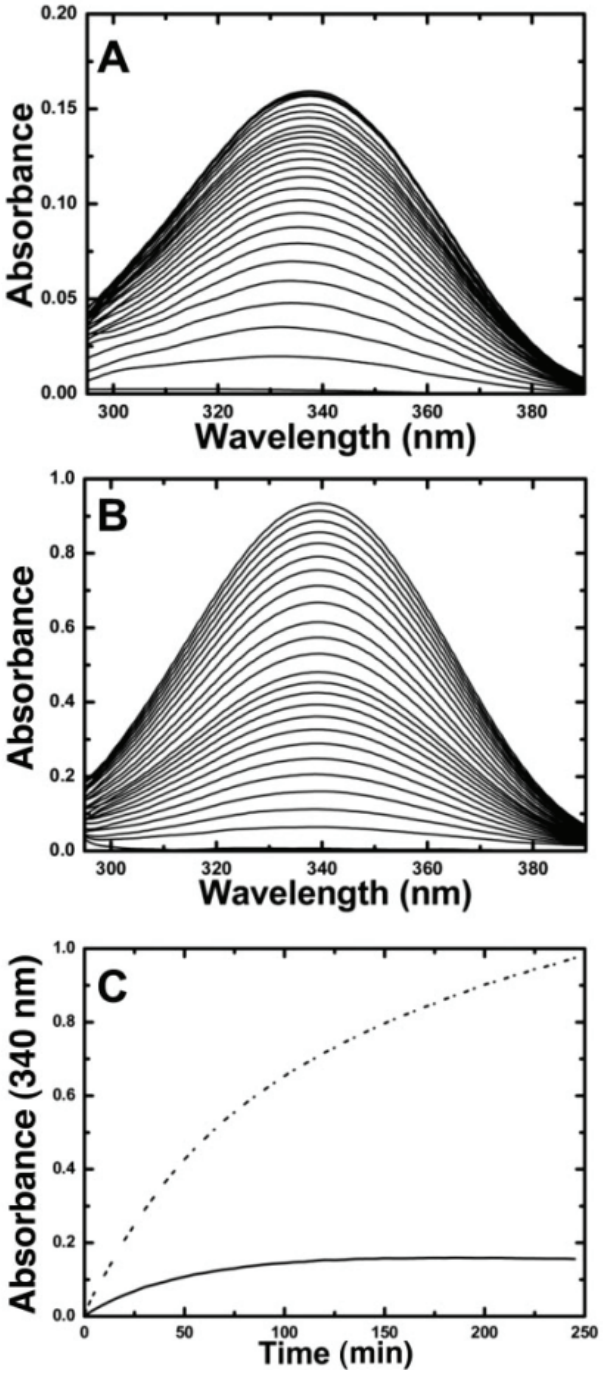

Figure. 5. Kinetic comparison of UGDH point mutants. Purified recombinant UGDH point mutant enzyme activity was assayed as conversion of NAD^+ to NADH detected by absorbance scans from 290 to 400 nm. Standard conditions used for wild type enzyme produced no activity from the mutant enzymes, so a time course was performed. *A*, C276S scans at 5-min intervals to 4 h. *B*, K279A scans at similar time points. *C*, absorbance at 340 nm was replotted over the time course of the assay to compare NADH appearance for C276S (*solid line*) and K279A (*dotted line*).

Table III
Rate constants for wild type and mutant UGDH

Enzyme	k_1	k_2
	mol/min/mg	*nmol/min/mg*
UGDH	110.7 ± 1.45	
C276S	2.69 ± 0.19	No activity
K279A	2.47 ± 0.11	0.396 ± 0.066

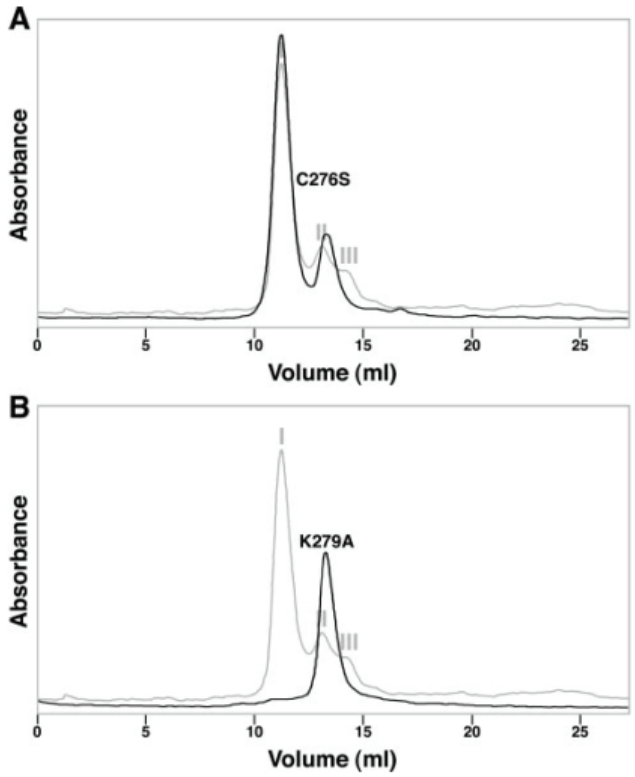

Figure 6. Size determination of UGDH point mutant structures. Molecular mass of the functional point mutant enzyme complexes was measured by FPLC as described under "Experimental Procedures" and in the legend to Figure 3. *A*, C276S superimposes on the wild type trace and is likely hexameric. *B*, K279A superimposes on the wild type dimer, indicating that this mutant is functioning predominantly as a dimer in kinetic assays.

date, only one such study has been done; cysteine 260 of *S. pyogenes* UGDH was converted to a serine, and the mutant lost activity but no quantitative data were published (24). Active site residues in the bovine enzyme have been identified by chemical modifications only. We sought to acquire mechanistic details for the human enzyme by a combination of site-directed mutagenesis, activity measurements, and homology modeling. Although only 23% identical to bacterial UGDH, the sequence of the human enzyme mapped well onto the crystal coordinates determined for the bacterial enzyme. By modeling the protein in this fashion, we were able to generate an image of the putative interactions within the active site of a ternary complex composed of human UGDH, NAD^+ cofactor, and UDP-glucose substrate (Figure 4). Inspection of this model, combined with identification of conserved residues in a primary sequence alignment of UGDH across diverse species and consideration of published data for the bovine and bacterial enzymes, directed us toward the selection of two key conserved amino acid residues likely to have a role in the catalytic mechanism: Cys-276 and Lys-279.

The figure illustrates a network of hydrogen bonding interactions within the active site that may serve to stabilize the ternary complex and facilitate catalysis. Lys-279 appears to bind the 3'-hydroxyl of the NAD^+ ribose (though mutation of that residue had no effect on our NAD^+ binding data) and forms an electrostatic interaction with Asp-280. Asp-280, in turn, positions a water molecule at the active site, thereby indirectly linking to NAD^+, the 6'-OH of the substrate, and Cys-276. This water molecule may be a structural edifice or a component of the reaction mechanism. It has been suggested that the water molecule would serve as a general base for proton abstraction during the first oxidation step in the bacterial reaction scheme (23).

Its central location at the active site then would be important to preserve and would depend on interactions donated by Lys-279 and Cys-276, but our data do not address this directly. The cysteine thiol thus positioned is within hydrogen bonding distance of the 6'-hydroxyl of UDP-glucose and is located appropriately for catalysis.

The mechanism proposed for bacterial UGDH involves the production of UDP-hexodialdose as an intermediate (21). Catalysis then is postulated to proceed via formation of a thiohemiacetal between Cys-276 and this intermediate, which is oxidized to a thioester before hydrolysis to yield the final carboxylate product. Our data demonstrate that Cys-276 is capable of a single NAD^+ reduction, which is consistent with this hypothesis. However, the hexodialdose intermediate never has been isolated either from the bacterial or the bovine reaction system. Instead, investigators of the bovine system postulated a reaction intermediate that was covalently linked to the enzyme and not released between oxidations (14). Ordman and Kirkwood (14) hypothesized a Schiff base intermediate that would be linked via an active site lysine. To demonstrate this and identify the enzyme residue linkage, these authors derivatized the putative active lysine with [^{14}C]formaldehyde and reduced with $NaBH_4$, thereby placing a mechanism-dependent label at the active site. These studies clearly suggest that the enzyme first forms a Schiff base linkage with the 6'-carbon of UDP-glucose, allowing the C-6'-hydroxyl subsequently to undergo the first oxidation, as we have depicted in Scheme 1. Our data using C276S also are consistent with this scheme. Interestingly, although Lys-279 appeared to be important for maximally efficient catalysis, its role is probably indirect: to constrain the position of an essential catalytic residue or the active site water. Accordingly, we have mutagenized an additional lysine, K220A, which entirely lacks enzymatic activity, implying that Lys-220 is an essential catalyst for the first oxidation of UDP-glucose and highlighting it as a candidate for the Schiff base intermediate. (B. J. Sommer, J. J. Barycki, and M. A. Simpson, manuscript in preparation.)

The collective summary of the studies described suggests to us the reaction mechanism as outlined in Scheme 1 with key residues we have identified illustrated in their respective roles. The reaction sequence is initiated by the binding of UDP-glucose, followed by NAD^+. Lys-220 forms a covalent linkage to the C-6' of UDP-glucose, the hydroxyl is lost as water, and the secondary amine is oxidized to a Schiff base between C-6' and Lys-220, releasing NADH. The thiol of Cys-276 simultaneously attacks C-6' as water hydrolyzes the Schiff base, forming a thiohemiacetal that is oxidized by reduction of a second NAD^+ to the thioester. Hydrolysis of the thioester releases the final UDP-glucuronic acid product. The mechanism suggests that specific inhibitors may be most effective at the level of Schiff base or thiohemiacetal formation because these would exploit the retention of covalent intermediates by the enzyme and be mechanistic inhibitors.

Acknowledgments

We thank Dr. Gloria Borgstahl (University of Nebraska Medical Center) for performing dynamic light scattering experiments.

References

1. Hacker, U., Lin, X., and Perrimon, N. (1997) *Development* **124,** 3565-3573
2. Hwang, H. Y., and Horvitz, H. R. (2002) *Proc. Natl. Acad. Sci. U. S. A.* **99,** 14224-14229
3. Walsh, E. C., and Stainier, D. Y. (2001) *Science* **293,** 1670-1673
4. Camenisch, T. D., Spicer, A. P., Brehm-Gibson, T., Biesterfeldt, J., Augustine, M. L., Calabro, A., Jr., Kubalak, S., Klewer, S. E., and McDonald, J. A. (2000) *J. Clin. Investig.* **106,** 349-360
5. Fraser, J. R., Laurent, T. C., and Laurent, U. B. (1997) *J. Intern. Med.* **242,** 27-33
6. Auvinen, P., Tammi, R., Parkkinen, J., Tammi, M., Agren, U., Johansson, R., Hirvikoski, P., Eskelinen, M., and Kosma, V. M. (2000) *Am. J. Pathol.* **156,** 529-536
7. Ropponen, K., Tammi, M., Parkkinen, J., Eskelinen, M., Tammi, R., Lipponen, P., Agren, U., Alhava, E., and Kosma, V. M. (1998) *Cancer Res.* **58,** 342-347
8. Aaltomaa, S., Lipponen, P., Tammi, R., Tammi, M., Viitanen, J., Kankkunen, J. P., and Kosma, V. M. (2002) *Urol. Int.* **69,** 266-272
9. Simpson, M. A., Wilson, C. M., and McCarthy, J. B. (2002) *Am. J. Pathol.* **161,** 849-857
10. Lapointe, J., and Labrie, C. (1999) *Endocrinology* **140,** 4486-4493
11. Spicer, A. P., Kaback, L. A., Smith, T. J., and Seldin, M. F. (1998) *J. Biol. Chem.* **273,** 25117-25124
12. Nelsestuen, G. L., and Kirkwood, S. (1971) *J. Biol. Chem.* **246,** 3824-3834
13. Ordman, A. B., and Kirkwood, S. (1977) *Biochim. Biophys. Acta* **481,** 25-32
14. Ordman, A. B., and Kirkwood, S. (1977) *J. Biol. Chem.* **252,** 1320-1326
15. Ridley, W. P., Houchins, J. P., and Kirkwood, S. (1975) *J. Biol. Chem.* **250,** 8761-8767
16. Schiller, J. G., Bowser, A. M., and Feingold, D. S. (1972) *Carbohydr. Res.* **25,** 403-410
17. Franzen, J. S., Ashcom, J., Marchetti, P., Cardamone, J. J., Jr., and Feingold, D. S. (1980) *Biochim. Biophys. Acta* **614,** 242-255
18. Franzen, J. S., Marchetti, P. S., and Feingold, D. S. (1980) *Biochemistry* **19,** 6080-6089
19. Franzen, J. S., Ishman, R., and Feingold, D. S. (1976) *Biochemistry* **15,** 5665-5671
20. Franzen, J. S., Kuo, I., Eichler, A. J., and Feingold, D. S. (1973) *Biochem. Biophys. Res. Commun.* **50,** 517-523
21. Campbell, R. E., Sala, R. F., van de Rijn, I., and Tanner, M. E. (1997) *J. Biol. Chem.* **272,** 3416-3422
22. Campbell, R. E., and Tanner, M. E. (1999) *J. Org. Chem.* **64,** 9487-9492
23. Campbell, R. E., Mosimann, S. C., van De Rijn, I., Tanner, M. E., and Strynadka, N. C. (2000) *Biochemistry* **39,** 7012-7023
24. Ge, X., Campbell, R. E., van De Rijn, I., and Tanner, M. E. (1998) *J. Am. Chem. Soc.* **120,** 6613-6614
25. Stewart, D. C., and Copeland, L. (1998) *Plant Physiol.* **116,** 349-355
26. Turner, W., and Botha, F. C. (2002) *Arch. Biochem. Biophys.* **407,** 209-216
27. Kelley, L. A., MacCallum, R. M., and Sternberg, M. J. (2000) *J. Mol. Biol.* **299,** 499-520
28. Huang, C. C., Couch, G. S., Pettersen, E. F., and Ferrin, T. E. (1996) *Pac. Symp. Biocomput.* **1,** 724